August 2007

Direct-current and radio-frequency characterizations of GaAs metal-insulator-semiconductor field-effect transistors enabled by self-assembled nanodielectrics

H C. Lin
Purdue University

S K. Kim
Purdue University

D Chang
Purdue University

Y Xuan
Purdue University

Saeed Mohammadi
School of Electrical and Computer Engineering, Purdue University, saeedm@purdue.edu

See next page for additional authors

Direct-current and radio-frequency characterizations of GaAs metal-insulator-semiconductor field-effect transistors enabled by self-assembled nanodielectrics

H. C. Lin, S. K. Kim, D. Chang, Y. Xuan, S. Mohammadi, and P. D. Ye[a)]
School of Electrical and Computer Engineering, Purdue University, West Lafayette, Indiana 47907 and Birck Nanotechnology Center, Purdue University, West Lafayette, Indiana 47907

G. Lu, A. Facchetti, and T. J. Marks[b)]
Department of Chemistry, Northwestern University, Evanston, Illinois 60208 and the Materials Research Center, Northwestern University, Evanston, Illinois 60208

(Received 31 May 2007; accepted 3 August 2007; published online 27 August 2007)

Direct-current and radio-frequency characterizations of GaAs metal-insulator-semiconductor field-effect transistors (MISFETs) with very thin *self-assembled organic nanodielectrics* (SANDs) are presented. The application of SAND on compound semiconductors offers unique opportunities for high-performance devices. Thus, 1 μm gate-length depletion-mode *n*-channel SAND/GaAs MISFETs exhibit low gate leakage current densities of $10^{-2}-10^{-5}$ A/cm^2, a maximum drain current of 260 mA/mm at 2 V forward gate bias, and a maximum intrinsic transconductance of 127 mS/mm. These devices achieve a current cutoff frequency (f_T) of 10.6 GHz and a maximum oscillation frequency (f_{max}) of 6.9 GHz. Nearly hysteresis-free I_{ds}-V_{gs} characteristics and low flicker noise indicate that a high-quality SAND-GaAs interface is achieved. © *2007 American Institute of Physics*. [DOI: 10.1063/1.2776013]

Replacing conventional Si or strained Si with high-performance compound semiconductors as conducting channels is one of the most attractive solutions to push the performance of nanoscale metal-oxide-semiconductor (MOS) transistors to the next level. The lack of high-quality and thermodynamically stable insulators on GaAs or other III-V compound semiconductors in general has prevented them from becoming serious competitors to Si complementary MOS technology. Research on dielectric layers and passivation suitable for III-V devices has led to an extensive literature[1,2] and includes many approaches. Some of the most studied techniques include sulfur passivation,[3] silicon interface control layer (Si ICL),[4–6] Ga_2O_3 generated by photowashing,[7] *in situ* molecular beam epitaxy (MBE) growth of $Ga_2O_3(Gd_2O_3)$,[8,9] *ex situ* atomic layer deposition (ALD) growth of Al_2O_3 and HfO_2,[10–12] wet oxidation of InAlP,[13] jet vapor deposition[14] of Si_3N_4, and ALD or physical vapor deposition of HfO_2+Si ICL.[15–17]

We have previously reported the high-performance GaAs metal-insulator-semiconductor field-effect transistors (MISFETs) fabricated using very thin biomembranelike *self-assembled nanodielectrics* (SANDs) as the insulating layer.[18] Nanoscopically well-defined SAND layers have high chemical and thermal stability, are smooth and adherent, and can be deposited at room temperature using simple wet chemical techniques. Moreover, GaAs MISFETs with nanoscale organic insulators are advantageous over their GaAs metal-semiconductor field-effect transistor (MESFET) counterparts since the organic insulator between gate and channel prevents gate leakage currents. Thin SANDs developed in the organic thin-film transistor field exhibit excellent insulating properties (with leakage current densities as low as 10^{-9} A/cm^2 with native SiO_2 on Si), large capacitances (up to ~2500 nF/cm^2), and a single-layer dielectric constant (k) of ~16, enabling low-voltage organic thin-film transistor functions.[19,20] In this letter, we report on detailed direct-current (dc) and radio-frequency (rf) characterizations of SAND-based GaAs MISFETs. We observe high-quality interface between SAND and GaAs by characterizing low frequency noise with an extracted Hooge constant of 8.6 $\times 10^{-5}$, and the excellent interface quality is further demonstrated by the lack of hysteresis in the I_{ds}-V_{gs} characteristics.

The GaAs MISFET devices reported in this letter employ an 800 Å Si-doped (4×10^{17}/cm^3) GaAs layer as the channel and a 1500 Å C-doped (5×10^{16}/cm^3) GaAs buffer layer on a p+GaAs substrate grown by metal-organic chemical vapor deposition (MOCVD), as illustrated in the inset of Fig. 1. Device isolation is achieved by oxygen implantation, followed by activation annealing performed simultaneously with Ohmic contact formation. Ohmic contacts are formed by e-beam deposition of Au/Ge/Au/Ni/Au multilayer and a lift-off process, followed by a 400 °C annealing in a nitrogen

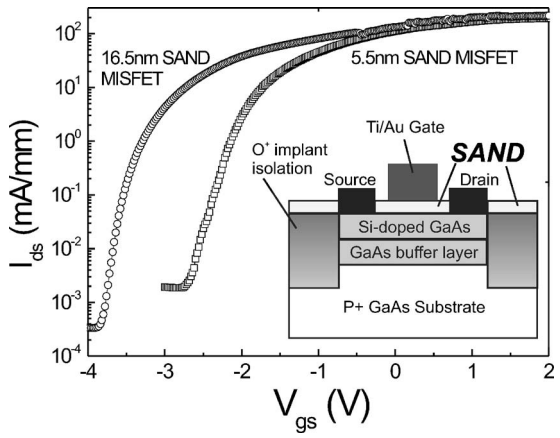

FIG. 1. Drain current vs gate bias for SAND/GaAs MISFETs at V_{ds} =3.0 V. Inset: schematic view of a depletion-mode *n*-channel GaAs MISFET with a self-assembled nanodielectric (SAND) as the insulating layer.

[a)]Electronic mail: yep@purdue.edu
[b)]Electronic mail: t-marks@northwestern.edu

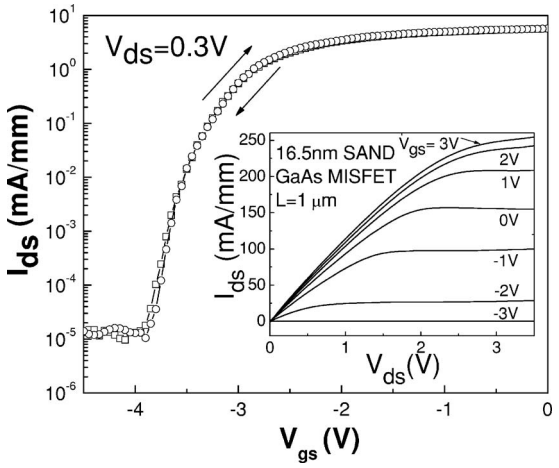

FIG. 2. Current I_{ds} vs V_{gs} as increasing (square) and decreasing (circle) gating sweeps for a 1 μm gate-length GaAs MISFET with a 16.5 nm thick SAND dielectric layer at V_{ds}=0.3 V. Inset: I_{ds} vs V_{ds} for the same device.

atmosphere. NH_4OH pretreatment is used to prepare hydrophilic GaAs surfaces prior to SAND deposition. The SAND deposition has been described previously.[18–20] For gate electrodes, Ti/Au metal deposition is carried out by e-beam evaporation, followed by lift-off.

The SAND films deposited on hydroxylated GaAs surfaces have two thicknesses 5.5 and 16.5 nm. The 16.5 nm thick SAND film is grown by three successive depositions of 5.5 nm thick SAND. The corresponding gate leakage current on a MISFET with a gate length of 1 μm and a gate width of 100 μm is very small, between 10 pA and 10 nA under V_{gs}=−4 V−+2 V at V_{ds}=3 V, and is at least six orders of magnitudes lower than the drain current. The dielectric strength of this organic film is as high as 6 MV/cm, which is comparable to that of conventional inorganic gate dielectrics such as SiO_2, Si_3N_4, or HfO_2. The multiple cross-linked Si–O layers in the SAND nanostructure significantly reduce the leakage current in the organic insulator and increase its maximum breakdown strength.[19,20] The I_{ds}-V_{gs} characteristics for 1 μm gate-length GaAs MISFETs with 5.5 and 16.6 nm SAND films are shown in Fig. 1. The 800 Å thick MOCVD GaAs channel layer leads to a maximum drain current of 260 mA/mm with pinch-off voltages of −2.6 V for 5.5 nm SAND and −3.7 V for 16.5 nm SAND, respectively. The pinch-off voltage is defined as the gate bias under V_{ds} =3 V when $I_{ds} \leqslant 0.01$ mA/mm. The sheet resistance and Ohmic contact resistance measured by the transmission length method are 2.5 kΩ/sq and 1.5 Ω mm, respectively. The maximum intrinsic transconductance g_m is ~127 mS/mm for the 5.5 nm SAND MISFET and ~101 mS/mm for the 16.5 nm SAND MISFET. The large transconductance values indicate that the interface trap densities are remarkably low. Note that the transconductance does not scale with the dielectric thickness because the devices are operating in depletion mode as opposed to surface channel devices.

Figure 2 shows the typical I_{ds} vs V_{gs} characteristics when V_{gs} is biased from −4.5 to 0.0 V and back to −4.5 V. The bidirectional gate-bias (V_{gs}) sweeps generate a hysteresis response indicating some threshold voltage drift. The amount of voltage shift has a significant dependence on the interface trap density at the SAND-GaAs interface. The nearly hysteresis-free response in the I_{ds} vs V_{gs} curves indicates low interface trap densities in this material system. The well behaved I_{ds} vs V_{ds} is also presented in the inset of Fig. 2. The calculated channel mobility for the MISFET with 16.5 nm SAND is ~1890 cm^2/V s.

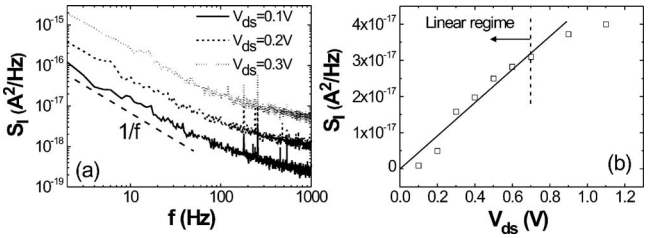

FIG. 3. (a) Excess $1/f$ noise spectra of a SAND-based GaAs MISFET. The device has 100×1 μm^2 gates and is biased at 0.1, 0.2, and 0.3 V on the drain and −3.0 V on the gate. (b) Drain current vs amplitude of current noise at f=100 Hz and a gate voltage of −3.0 V.

To evaluate the interface quality of the present GaAs MISFETs, we have measured the low frequency noise $(1/f)$ spectral density of the drain in the transistor linear operating regime and have extracted the value of Hooge's constant α_H. A low frequency noise was swept in the frequency range from 1 Hz to 1 KHz with the source terminal grounded. Figure 3(a) shows the drain current noise spectrum at a gate voltage of −3.0 V and drain voltages of 0.1, 0.2, and 0.3 V in the linear region of the I_{ds}-V_{ds} curve. At a constant gate bias, the drain current noise spectrum varies as $f^{-\beta}$, where β is close to 1 within 8%, and is therefore referred to as the $1/f$ noise. The governing Hooge equation for $1/f$ noise in a resistor is given by[21]

$$\frac{S_I(f)}{I_{ds}^2} = \frac{\alpha_H}{fN}, \tag{1}$$

where $S_I(f)$ is the current spectrum, N is the number of carriers, and α_H is a constant typically $\sim10^{-3}$ in bulk materials. The value of α_H can be used as a parameter to compare interface trap densities in devices regardless of the specific device parameters.[22,23] For a MISFET channel operating in the linear regime, the drain current can be expressed as

$$I_{ds} = \frac{q\mu N V_{ds}}{L^2}, \tag{2}$$

where q is the elementary charge, μ is the channel mobility, and L is the channel length. Combining Eqs. (1) and (2), one can calculate the current fluctuation in a MISFET operating in the linear regime as a function of drain current

$$S_I(f) = \frac{q\mu\alpha_H I_{ds} V_{ds}}{fL^2}. \tag{3}$$

Figure 3 shows the measured amplitude of current noise as a function of drain voltage V_{ds} at 100 Hz. The excess $1/f$ current noise spectrum of the GaAs MISFET with SAND is linearly proportional to the drain voltage in the linear regime. The extracted α_H is 2.6×10^{-4} for the 16.5 nm SAND-GaAs MISFET at V_{gs}=−3 V. Table I shows the α_H values for the present SAND-based GaAs MISFETs compared with previously published data for Si MOSFETs having HfO_2 dielectric and metal gates,[24] conventional NEC GaAs MESFETs,[22] and MBE-grown GaAs MESFETs.[22] The α_H value in the present SAND-based devices is comparable to those of commercial GaAs MESFET devices and superior to those of HfO_2/Si MOSFETs. This result clearly demonstrates that SAND can

TABLE I. Hooge parameter α_H on different types of devices.

Device	Hooge parameter α_H
MBE GaAs MESFET $(1\times 300\ \mu m)^2$	7.6×10^{-5}
MEC MESFETs (NE244)	5.6×10^{-5}
HfO_2 and metal gate Si MOSFET	1.0×10^{-3}
GaAs MISFET with SAND	2.6×10^{-4}

be utilized as the gate dielectric for high-quality interfaces on GaAs substrates.

The rf performance of SAND/GaAs MISFETs was also characterized with cutoff frequencies measured beyond 10 GHz. The rf characteristics are measured in an ambient environment using 8722D network analyzer and on-wafer probing techniques. Devices were biased using bias tees and were measured up to 30 GHz. The rf calibration technique utilizes multiple averaging with short-open-load-thru standards. This type of rf measurement can be performed with sufficient accuracy only if the parasitic components of the transistor pads are carefully removed from the intrinsic transistor structure. To obtain the intrinsic cutoff frequency (f_T) and maximum oscillation frequency (f_{max}) of the SAND-based GaAs MISFETs, *S* parameters of both device and probe pads were measured under different bias conditions, and de-embedding was carried out using the techniques described previously.[25] The f_T and f_{max} are determined by forward current gain (H_{21}) and maximum unilateral transducer power gain (G_u) extracted from the *S* parameters under different bias conditions. Figure 4 shows the maximum f_T and f_{max} values achieved for a 1 μm gate-length GaAs MISFET device with 5.5 nm thick SAND layer under biases of $V_{ds}=3.0$ V and $V_{gs}=0.1$ V. A peak f_T of 10.6 GHz and a peak f_{max} of 6.9 GHz are obtained, as shown in Fig. 4, within the reasonable frequency response range for 1 μm GaAs devices. The inset of Fig. 4 presents the summary of all f_T and f_{max} obtained as a function of V_{gs} at $V_{ds}=3.0$ V.

In conclusion, we have demonstrated the use of SAND nanodielectrics for high-speed GaAs MISFET devices exhibiting excellent transistor characteristics and high-quality interfaces on GaAs substrate. These results suggest good opportunities for manipulating the complex GaAs surface chemistry with unprecedented material options and for using organic dielectrics for high-performance III-V semiconductor devices. The SAND process is flexible, low cost, and far simpler to implement than the previously reported MBE or ALD dielectric deposition processes.

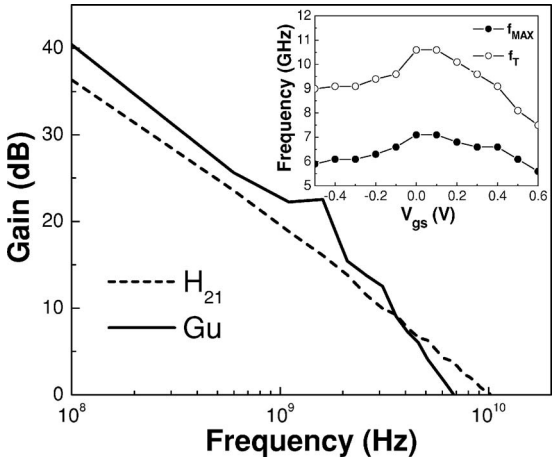

FIG. 4. Plot of maximum current gain (H_{21}) and maximum unilateral transducer power gain (G_u) as a function of frequency for a GaAs MISFET with a SAND thickness of 5.5 nm and a gate length of 1 μm at $V_{ds}=3$ V and $V_{gs}=0.1$ V. The extracted unity gain frequency f_T is 10.6 GHz and f_{max} is 6.9 GHz. Inset: rf response as a function of the gate voltage of a $1\times 100\ \mu m^2$ gate dimension SAND-based GaAs MISFET.

The authors thank the DARPA/ARO (W911NF-05-0187), the NASA Institute for Nanoelectronics and Computing (NCC 2-3163), the NSF (Grant No. ECS-0621949), and the SRC MARCO MSD Focus Center for the support on this research.

[1] T. Mimura and M. Fukuta, IEEE Trans. Electron Devices **ED-27**, 1147 (1980), and references therein.
[2] *Physics and Chemistry of III-V Compound Semiconductor Interfaces*, edited by C. W. Wilmsen (Plenum, New York, 1985), and references therein.
[3] B. J. Skromme, C. J. Sandroff, E. Yablonovitch, and T. Gmitter, Appl. Phys. Lett. **51**, 2022 (1987).
[4] G. G. Fountain, R. A. Rudder, S. V. Hattangady, R. J. Markunas, and J. A. Hutchby, Tech. Dig. - Int. Electron Devices Meet. **1989**, 887.
[5] M. Akazawa, H. Ishii, and H. Hasegawa, Jpn. J. Appl. Phys., Part 1 **30**, 3744 (1991).
[6] D. S. L. Mui, H. Liaw, A. L. Demirel, S. Strite, and H. Morkoc, Appl. Phys. Lett. **59**, 2847 (1991).
[7] S. D. Offsey, J. M. Woodall, A. C. Warren, P. D. Kirchner, T. I. Chappell, and G. D. Pettit, Appl. Phys. Lett. **48**, 475 (1986).
[8] M. Passlack, M. Hong, and J. P. Mannaerts, Appl. Phys. Lett. **68**, 1099 (1996).
[9] M. Hong, J. Kwo, A. R. Kortan, J. P. Mannaerts, and A. M. Sergent, Science **283**, 1897 (1999).
[10] P. D. Ye, G. D. Wilk, J. Kwo, B. Yang, H.-J. L. Gossmann, M. Frei, S. N. G. Chu, J. P. Mannaerts, M. Sergent, M. Hong, K. Ng, and J. Bude, IEEE Electron Device Lett. **24**, 209 (2003).
[11] P. D. Ye, D. G. Wilk, B. Yang, S. N. G. Chu, K. K. Ng, and J. Bude, Solid-State Electron. **49**, 790 (2005).
[12] M. M. Frank, G. D. Wilk, D. Starodub, T. Gustafsson, E. Garfunkel, Y. J. Chabal, J. Grazul, and D. A. Muller, Appl. Phys. Lett. **86**, 152904 (2005).
[13] X. Li, Y. Cao, D. C. Hall, P. Fay, B. Han, A. Wibowo, and N. Pan, IEEE Electron Device Lett. **25**, 772 (2004).
[14] W. P. Li, Y. X. Liu, X. W. Wang, and T. P. Ma, *Proceedings of the 36th IEEE Semiconductor Interface Specialists Conference*, Washington DC, December 2005 (unpublished).
[15] S. Oktyabrsky, V. Tokranov, M. Yakimov, R. Moore, S. Koveshnikov, W. Tsai, F. Zhu, and J. C. Lee, Mater. Sci. Eng., B **135**, 272 (2006).
[16] I. Ok, H. Kim, M. Zhang, T. Lee, F. Zhu, L. Yu, S. Koveshnikov, W. Tsai, V. Tokranov, M. Yakimov, S. Oktyabrsky, and J. C. Lee, Tech. Dig. - Int. Electron Devices Meet. **2006**, 829.
[17] Y. Sun, S. J. Koester, E. W. Kiewra, K. E. Fogel, D. K. Sadana, D. J. Webb, J. Fompeyrine, J.-P. Locquet, M. Sousa, and R. Germann, *Conference Digest of the 64th Device Research Conference*, 2006 (unpublished), p. 49.
[18] H. C. Lin, P. D. Ye, Y. Xuan, G. Lu, A. Facchetti, and T. J. Marks, Appl. Phys. Lett. **89**, 142101 (2006).
[19] M. H. Yoon, A. Facchetti, and T. J. Marks, Proc. Natl. Acad. Sci. U.S.A. **102**, 4678 (2005).
[20] M. H. Yoon, H. Yan, A. Facchetti, and T. J. Marks, J. Am. Chem. Soc. **127**, 10388 (2005).
[21] F. N. Hooge, Phys. Lett. **29A**, 139 (1969).
[22] K. H. Duh and A. van der Ziel, IEEE Trans. Electron Devices **ED-32**, 662 (1985).
[23] G. Ghibaudo, O. Roux, C. Nguyen-Duc, F. Balestra, and J. Brini, Phys. Status Solidi A **124**, 571 (1991).
[24] B. Min, S. P. Devireddy, Z. Celik-Butler, F. Wang, A. Zlotnicka, H. Tseng, and P. J. Tobin, IEEE Trans. Electron Devices **51**, 1979 (2004).
[25] E. P. Vandamme, D. M. M.-P. Schreurs, and C. van Dinther, IEEE Trans. Electron Devices **48**, 737 (2001).